We are IntechOpen, the world's leading publisher of Open Access books Built by scientists, for scientists

4,800
Open access books available

122,000
International authors and editors

135M
Downloads

Our authors are among the

154
Countries delivered to

TOP 1%
most cited scientists

12.2%
Contributors from top 500 universities

CLARIVATE ANALYTICS BOOK CITATION INDEX INDEXED

WEB OF SCIENCE™

Selection of our books indexed in the Book Citation Index in Web of Science™ Core Collection (BKCI)

Interested in publishing with us?
Contact book.department@intechopen.com

Numbers displayed above are based on latest data collected.
For more information visit www.intechopen.com

12

Microwave and Millimeter Wave Technologies A New X-Band Mobile Direction Finder

Sergey Radionov[1], Igor Ivanchenko[1], Maksym Khruslov[1], Aleksey Korolev[2] and Nina Popenko[1]
[1] *Usikov Institute for Radiophysics and Electronics of the National Academy of Sciences of Ukraine*
12 Ak. Proskura St., Kharkov, 61085, Ukraine
ireburan@yahoo.com
[2] *Institute of Radioastronomy of the National Academy of Sciences of Ukraine*
4 Krasnoznamennaya st., 61085, Kharkov, Ukraine

1. Introduction

Nowadays, the radio direction finding (DF) has numerous applications in a variety of fields such as radio monitoring, navigation, disaster response, wildlife tracking, electronic warfare [Poisel, 2005], and personal locating service [Xiaobo & Zhenghe, 2002]. DF also forms an important branch of electronic intelligence. With the aim to get high resolution, a large baseline is usually used. In this case the most common DF approach uses phase interferometry method in which the phase delay across the array length (baseline) is measured. Many of DF techniques such as interferometer, correlative interferometer and multiple signal classification [Jnkins, 1991; Schmidt, 1986; Jun-Ho Choi et al., 2008] use the phase information to estimate the angle of arrival. It is well-known that increasing the element spacing increases the resolution, but also proportionally increases the phase ambiguities that must be resolved. These ambiguities occur when the spacing between antenna elements is greater than half of the signal wavelength. As a result of this, multiple baselines are commonly used to resolve ambiguities in DF systems [Pace, 2001; Kwai et al., 2008]. However, there is a need to take into account that the presence of unknown mutual coupling between array elements degrades significantly the performance of most high-resolution DF algorithms. Therefore, many array calibration methods have treated mutual coupling calibration as a parameter estimation problem [Friedlander & Weiss, 1991; See & Poh, 1999; Bu-hong et al., 2008]. It is appropriate mention here that fairly often the DF systems use very small individual radiators with degraded gain when the overall dimensions are important in contrast to the DF antennas in telecommunications systems, where gain or directivity is a prime requirement [Peyrot-Solis et al., 2005; Schantz, 2004; Chevalier et al., 2007]. As regards the wireless communications, during last decade the radio systems operating at frequencies higher 1GHz are widely used. Among them we can point

out the broadband radio-modems with data transmission rate higher 2Mbit/sec. The operational frequencies of those are usually found to be in limits ranging from 1GHz to 5.8GHz. At the same time the advancement to the state-of-the-art backbone links (for instance, WiMAX standards-based technology) compels moving to the higher frequencies. With these remarks in mind a problem of bearing, for example, the unauthorized local SHF sources becomes a topical question and there is a need of suitable broad-band mobile DF. In this respect we can note the compact dually polarized direction finding antenna system, working in the 500–3000MHz frequency band [Bellion et al., 2008] and hand held antenna array for localization of radio devices working on TETRA frequency ranges (380-390 MHz) [Sarkis et al., 2008].
The main objective of this paper is developing and designing X-band hand held DF system for localization the local SHF sources by using the "null-amplitude" technique.

2. Design and Experimental Technique

There is a set of canonical radiators, which are used as the individual antennas or the elementary radiators deployed in different array configurations. Here, the researchers offer and utilize various modifications of such the radiators to overcome the problems in the field of the state-of-the-art electromagnetics. Among a majority of individual radiators we have given preference to the usual cylindrical monopole antenna due to its simplicity of designing, omnidirectional radiation pattern in azimuth plane, broadbandness, as well as high values of the antenna gain and efficiency. In the process of our earlier comprehensive investigations of different radiators it has been found that the radiation characteristics of the cylindrical monopole antenna can be sufficiently changed by means of choice the suitable correlations between the monopole height and ground plane size [Ivanchenko et al., 2006; Khruslov & Pazynin, 2006]. In this respect, the revealed opportunity to produce the mono-beam conical radiation pattern with the high elevation angle of the peak directivity and relatively small ground plane of antenna attracted our attention especially. Just this result suggested us to apply such a monopole antenna as a sub-reflector of the reflector-type antenna for the DF [Ivanchenko et al., 2007; Radionov et. al. 2007; Ivanchenko et al., 2008]. Here, it should also be noted that in this case unlike the well-known reflector-type antenna with a dipole vibrator, the proposed antenna allows for connecting the sub-reflector directly to the standard 50 Ohm impedance coaxial feeder.
In this case the most preferable "null-amplitude" technique of the received signal should be applied. As a result of this, the following characteristics of the DF antenna should be provided, namely:

- we have to have the relatively narrow mono-beam conical radiation pattern;
- the elevation angle of the peak directivity should be as much as closer to zenith;
- the power ratio of signal in the antenna axis and in the direction of the radiation maximum as well as the power level of side lobes should at least be less than –10dB;
- the antenna should be essentially broadband one.

It is quite clear that in an effort to achieve the aforementioned characteristics of the reflector antenna, the radiation characteristics of the sub-reflector will have a defining value. Therefore, the main question we address is a choice of the optimal geometry of the monopole antenna from the point of view of designing a compact reflector antenna.

The experiments were carried out in the reactive, radiating and far-field regions of the monopole antennas differing by the monopole height and ground plane size. These experiments were performed with the help of the methods, facilities and special probes developed and designed in the Laboratory of High Frequency Technology and described in detail in our earlier papers [Ivanchenko et al., 2002; Cao et al., 2002; Andrenko et al., 2006; Chernobrovkin et al., 2006; Chernobrovkin et al., 2007]. As an example, the near-field distributions of the quarter-wave monopole antenna with different ground plane radii are shown in Fig. 1a. Thick solid lines at the bottom of pictures show the ground plane size of the monopole antenna. The EM field distributions in the far-field region were measured in the sweep mode of the SHF oscillator that allows for analysing the radiation pattern behaviour in the frequency band of interest. The respective far-field pictures of antenna in coordinates "frequency-radiation angle", where the colour spectrum corresponds to the EM field power distribution, are presented in Fig. 1b.

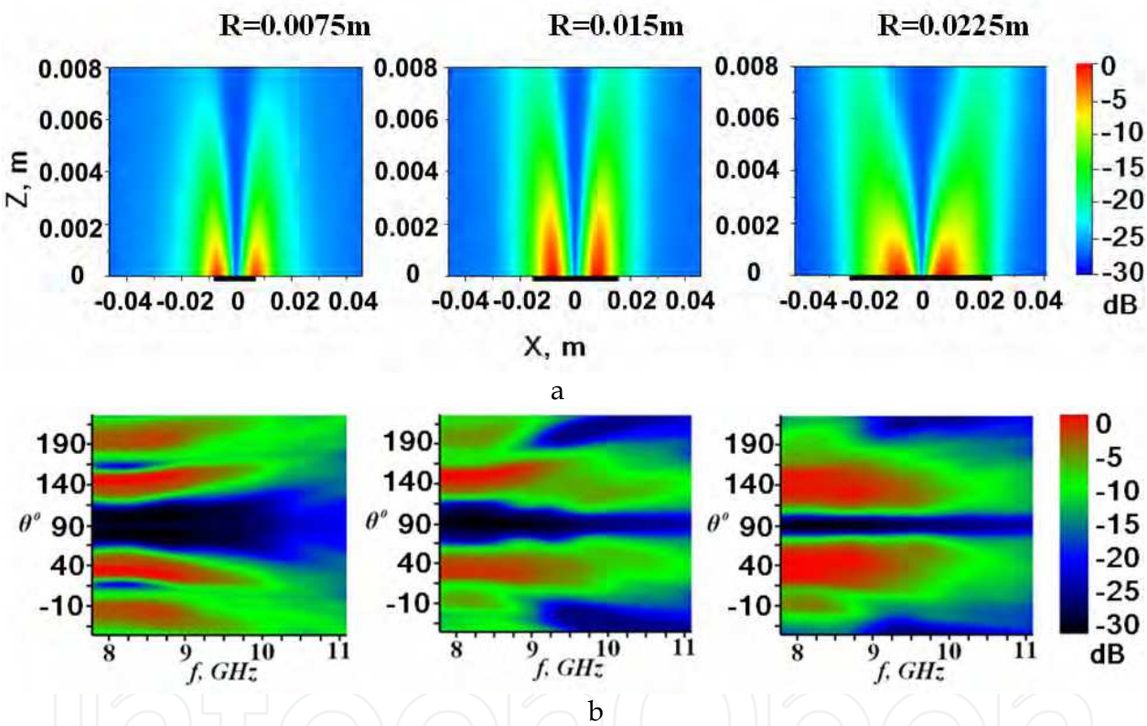

Fig. 1. Near-field distributions (a) and radiation patterns (b) of the quarter-wave cylindrical monopole antenna

3. Optimization of the Reflector Antenna

The vertical monopole as an extension of the central conductor of the coaxial cable with diameter 2b=0.0014m is located above the circular metallic ground plane with thickness d=0.0005m (Fig. 2). We focus on the two monopole heights *h*, namely: quarter-wavelength (h=λ/4) and three fourth-wavelength (h=3λ/4) monopoles (the wavelength λ=0.030m). The ground plane radius R varies from 0.0075m to 0.0375m with the step of 0.0075m. The input reflection coefficient S_{11}, near-field distributions in the reactive region, radiation patterns, and antenna bandwidth are the characteristics for our analysis. The near-field distributions

in the reactive region are performed on the set-up described in [Ivanchenko et al., 2002]. The scan area in the XOY plane is adjusted to the ground plane size and located at the stand-off distance of 0.001m above the ground plane surface.

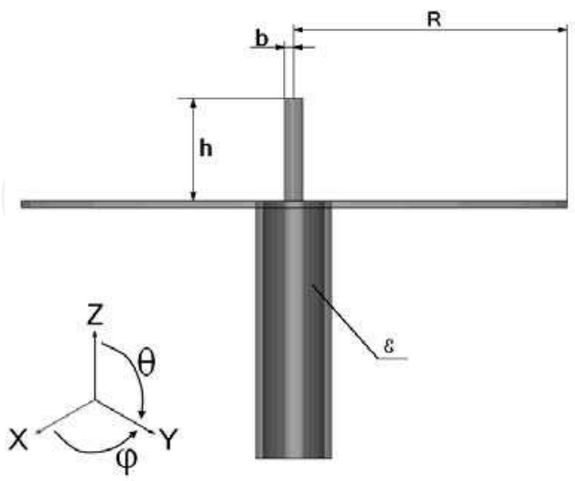

Fig. 2. Schematic view of the monopole antenna

The results obtained in the process of measuring the EM field distributions in the reactive region of the quarter-wavelength monopole antenna show that the field distributions of the Hφ-component have two variations along the ground plane radius which equal to an integer number times λ/2 (Fig. 3a and Fig. 3b). In this case the first maximum of the magnetic field component is observed near the antenna center, the first minimum of the magnetic field is located at the distance ≈λ/4 from the ground plane edge, and the second maximum is located outside the ground plane edge. At the same time, the antennas with ground plane radii equal to the odd number times λ/4 (Fig. 3c) have more than one oscillation along the ground plane radius thereby pointed out the interference nature of the fields in the close vicinity of the ground plane surface.

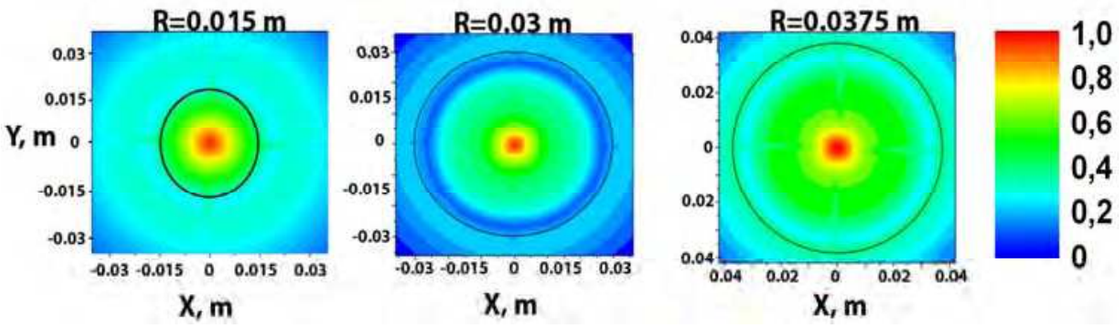

a b c

Fig. 3. Near-field distributions of the Hφ-component measured in the reactive region of antennas with h=λ/4 and different ground plane radii: R=0.015m (a); R=0.030m (b), and R=0.0375m (c) .The black circles on the pictures show the ground plane size

The regularities revealed in the near-field distributions should also be reflected in the antenna beam pattern. In fact, the simulated radiation pattern shape of antennas undergoes

appropriate changes when increasing the ground plane radius (Fig. 4). In particular, the secondary beams appear in the backward direction of antennas with the ground plane radii R≥0.030m and in the broadside direction of antennas with the ground plane radii R≥0.0375m. The elevation angle of the peak directivity of antennas with different substrate radii R is oriented at $\theta=60^0$ (R=0.015m), $\theta=60^0$ (R=0.03m), and $\theta=54^0$ (R=0.0375m). It is the author's opinion that these changes in the elevation angle are just determined by the different EM distributions in the reactive region of antennas noted above (Fig. 3).

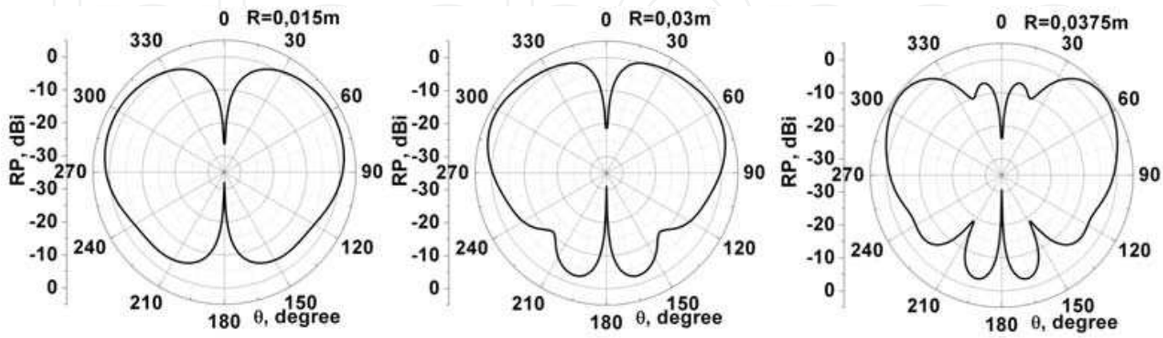

Fig. 4. Simulated radiation patterns of antennas with *h=λ/4* and different ground plane radii: R=0.015m (a); R=0.030m (b), and R=0.0375m (c)

Unlike the antenna with h=λ/4 (Fig. 4) the monopole antenna with h=3λ/4 produces mono-beam radiation pattern in the broadside direction without evident pattern shape transformations when increasing the ground plane radius (Fig. 5). However, the radiation patterns become the multi-beam ones in the backward direction though a power level of the lobes is substantially smaller than that of the antenna with h=λ/4. The elevation angle of the peak directivity of antennas with substrate radii R>0.0225m is virtually the same, namely: θ=430 (R=0.015m), θ=330 (R=0.0225), and θ=340 (R=0.03m). The measured radiation patterns are in good agreement with simulated ones.

In the framework of these investigations some general regularities in the radiation pattern formation for both monopole heights have been determined, namely: (i) the differences in the near-field distributions lead to the changes in both the radiation pattern shape and the elevation angle of the peak directivity when varying the ground plane radius; (ii) the additional lobes in the broadside and backside directions appear when increasing the ground plane radius; (iii) the influence of the ground plane size on antenna performance is less for antennas with the monopole height h=3λ/4 than that for antennas with the monopole height h=λ/4. As it should be from measurements of near-fields and radiation patterns the monopole antenna with parameters h=0.0075m and R=0.015m seems to be the entirely acceptable one as the sub-reflector because the wave beam is to be wide enough for the effective illumination of the main reflector and the ground plane size is sufficiently small.

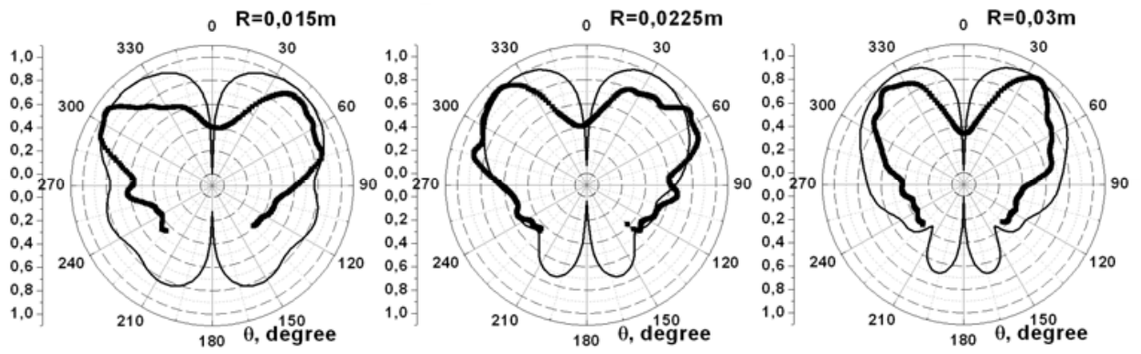

a b c

Fig. 5. Simulated (thin line) and measured (thick line) radiation patterns of antennas with h=3λ/4 and different ground plane radii: R=0.015m (a); R= 0.0225m (b), R= 0.030m (c)

The geometrical parameters of the DF antenna consisting of the parabolic reflector and monopole antenna as a primary source are shown in Fig. 6. The primary source is fixed in the foam box and the distance D between the monopole and the reflector can be changed during the experiment.

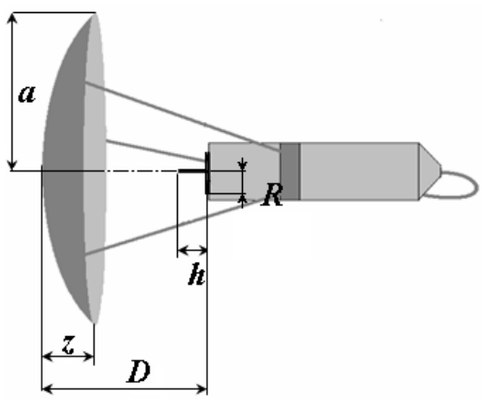

Fig. 6. Schematic view of the reflector antenna.

First, we have carried out a computational modeling of the reflector antenna with the following parameters of sub-reflector: h=0.075mm and R=0.015m. From our study it has been found that the radiation pattern demonstrates the high level of side lobes (Fig. 7a). Therefore, we have proceeded with computational modeling of the reflector antenna by varying its geometrical parameters in the following limits: 0,015m<R<0.0375m, 0.05m<a< 0.100m, and 0.04mm<D<0.06m for the two monopole heights h=0.0075m and h=0.0225m (Fig. 6) with the aim to optimize the reflector antenna prototype from the point of view of the main reflector blockage and the utilization factor of its surface. Furthermore, we have to take into account that the antenna should be a long-focus one (D>2a/4) in order to minimize the cross-polarization level and to provide a good matching of antenna with a feeding line in the wide frequency band. As a result of investigations the optimal parameters of the reflector antenna have been determined, namely: the aperture radius of the main reflector is a=0.080m, the monopole height h=0.0225m, the ground plane radius R=0.0225m, the focal

length of the parabolic reflector D=0.055mm. As can be seen from the Fig. 7b, the simulated radiation pattern of the reflector antenna with aforementioned parameters shows substantially lower level of side lobes.

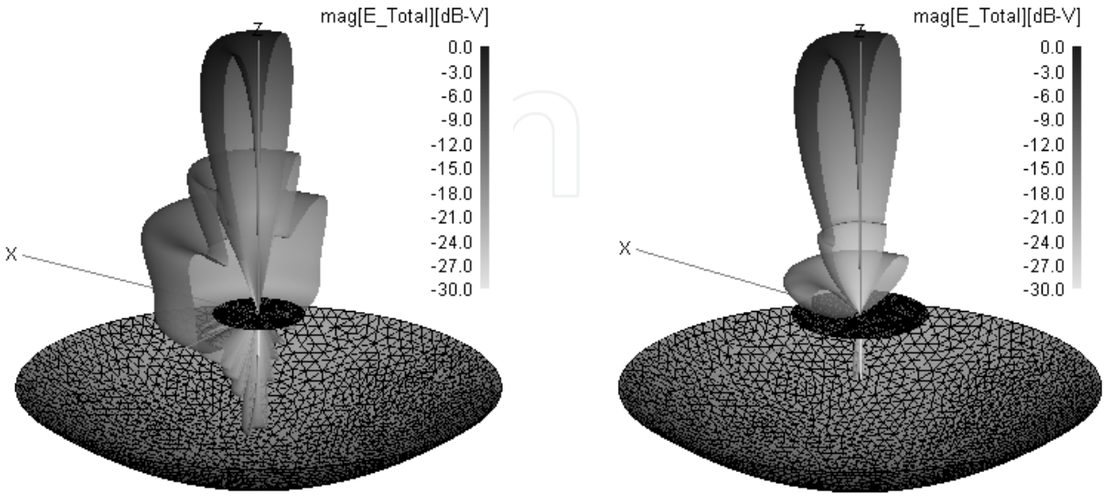

a b

Fig. 7. Simulated radiation patterns of the reflector antenna with h=0.0075m, R=0.015m (a) and h=0.0225mm, R=0.0225mm (b) parameters.

The characteristics of the reflector antenna (θ^0 is the elevation angle; $\Delta\theta^0$ is the beamwidth) are shown in Table 1. The angle $\Delta\theta'$ is determined by the two positions of the DF antenna relative to the external SHF source when the signal amplitude increases on 3dB in comparison with the signal level in the "global" minimum of the radiation pattern.

θ (degree)	Δθ (degree)	Δθ' (degree)	Side lobe level (dB)	Gain (dB)
Theory				
10	10	1.5	-21	18
Experiment				
10	7	1.5	-19	17

Table 1. The characteristics of the reflector antenna

With these remarks in mind we have manufactured the novel reflector-type antenna. The measured VSWR of the antenna prototype is less than 2 in the wide frequency band (Fig. 8).

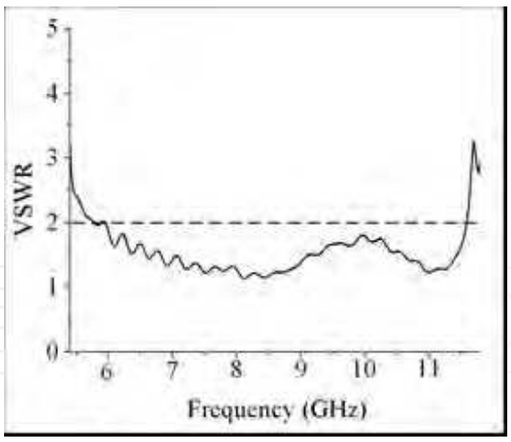

Fig. 8. VSWR of the antenna prototype

With the aim to study the process of radiation shaping of the reflector antenna and to optimize the mutual arrangement of supporting elements, we have carried out the simulations and measurements of EM field distributions in the radiating region of the reflector antenna prototype. The near-field distribution being measured at frequency f=10GHz is shown in Fig. 9a for the optimized DF antenna prototype. As one sees from this picture, one has the main lobe and the weak side lobe with a power level around -15dB. The simulations of near-field distribution at the same frequency f=10GHz (Fig. 9b) points out a qualitative agreement with the experiment. Thus, we can pronounce that the selected by us supporting elements do not virtually disturb the EM field distribution in the radiating region of the antenna prototype.

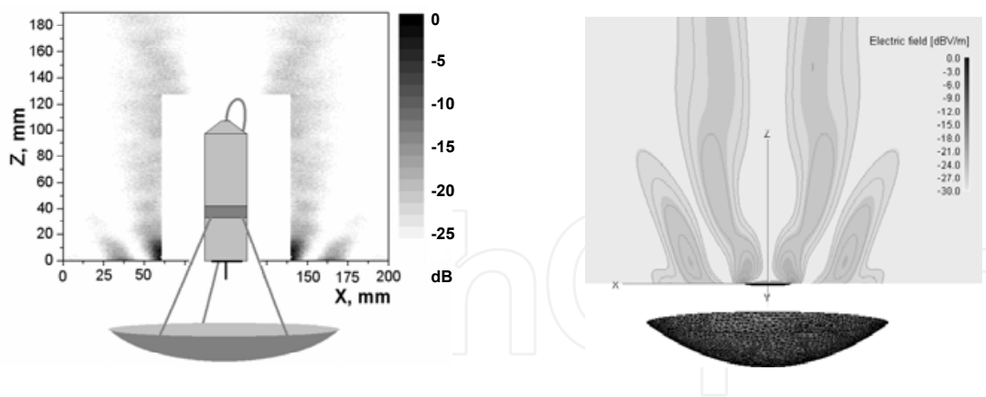

a b

Fig. 9. Measured (a) and simulated (b) near-field distributions of the antenna prototype

The experiments being performed in the far-field region of the DF antenna have shown that the antenna produces mono-beam conical radiation pattern in the bandwidth of 5.5GHz (Fig. 10a) with the elevation angle of the peak directivity equals to 10^0 and the beamwidth around 10^0. We note that the radiation pattern shape remains virtually the same within the antenna bandwidth. The typical radiation pattern at frequency f=10GHz is shown in Fig. 10b. From the practical point of view it is important that the power signal ratio in the

antenna axis and in the main lobe maximum is less than -20dB. It should be also noted that the principal characteristic of the DF using the "null-amplitude" technique is the angular domain of the "global" minimum of the radiation pattern Δθ' which equals to 1.50 in this case.

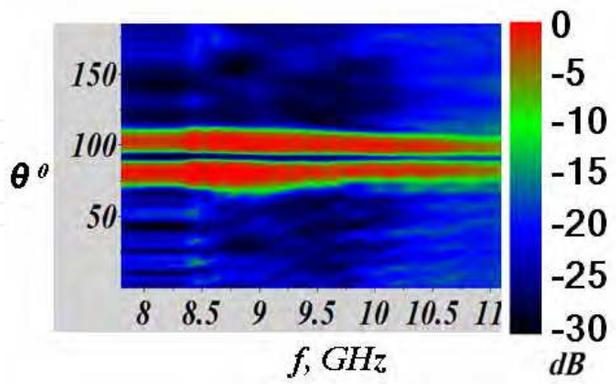

a

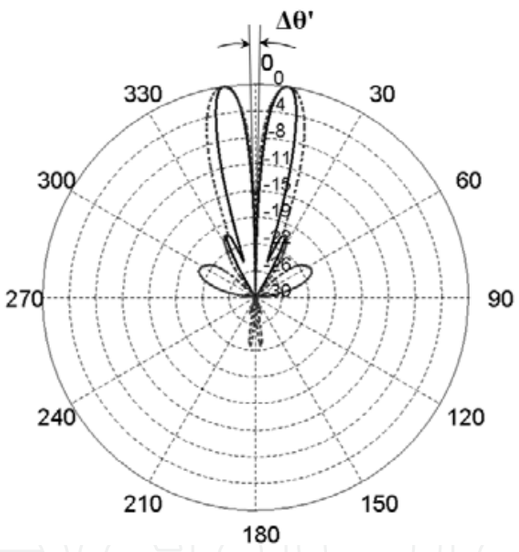

b

Fig. 10. Measured radiation pattern within the antenna bandwidth (a); simulated (dotted line) and measured (solid line) radiation patterns at f=10GHz (b) of the antenna prototype

Thus, the reflector antenna has the good principal characteristics such as elevation angle, beamwidth, bandwidth, and sharp power minimum along the antenna axis that allows us to expect high sensitivity and space resolution of the proposed DF.

4. Direction Finder Prototype

The conceptual diagram of the DF is shown in Fig. 11a. The signal received from the SHF source enters into the low-noise amplifier for the signal pre-amplification over the entire operational frequency band. The subsequent logarithmic amplifier realizes the signal amplification to the level to be quite enough for the effective ultra wideband video detector operation (U=1mV) and provides a suitable dynamic range of the received signal thereby guarantees a high accuracy of the center of "global" minimum location. The need in the UWB detector is determined by a large difference (up to 20dB) of the signal power in the main lobe and in the "global" minimum of the radiation pattern. The wideband low-noise video amplifier with a small integration time constant (τ=0,1 – 1 microseconds for the choice) increases the signal up to the level required to the stable flash encoder operation (around 2.5V). The photo of the DF prototype is shown in Fig. 11b.

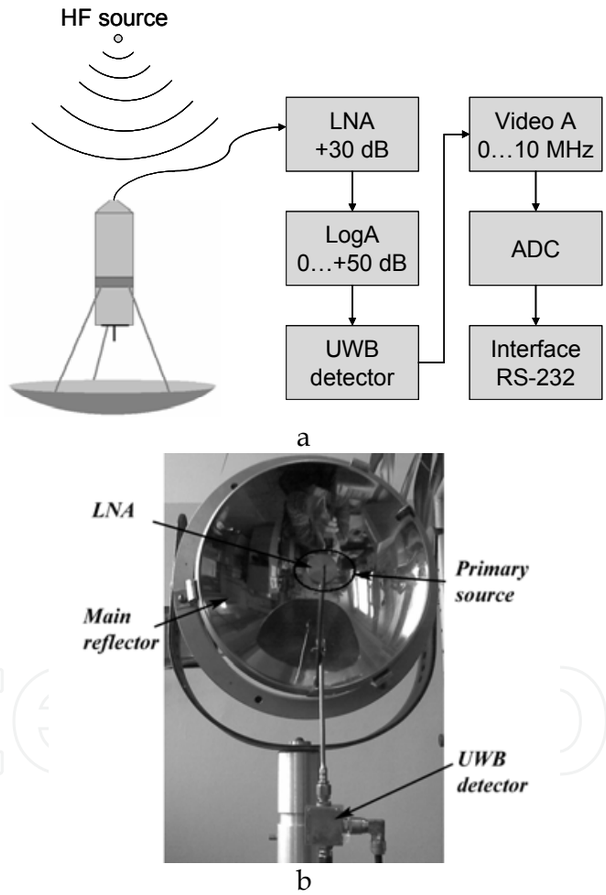

Fig. 11. Block-diagram of the direction finder (a) and direction finder prototype (b)

After video-amplifier the signal enters the interface, which serves for the registration, numeralization, and displaying the level of received signal, and than enters the working board of the control unit. The photo of the control unit is shown in Fig. 12a. As the radiation pattern looks like a "bell" shape we imitate a bearing process on the front panel of the

control unit by V-symbol of the light emitting diodes (LED) which are connected with the power level of the received signal (Fig. 12b).

a

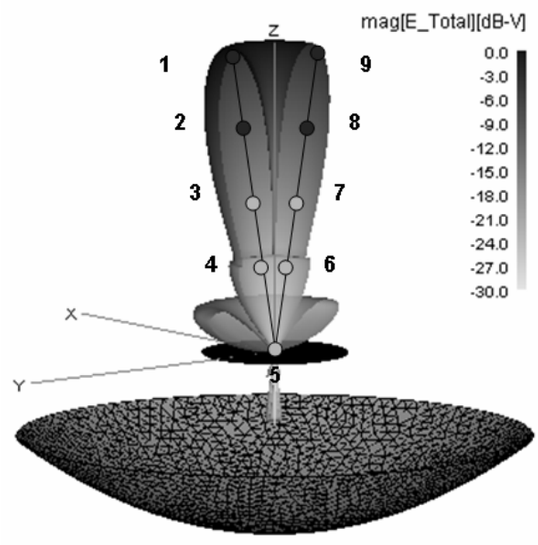

b

Fig. 12. Control unit (a) and conformity of the bearing process indication (b)

5. The Bearing Algorithm

The bearing algorithm is as follows. It is quite clear that first of all the preliminary scan of the space area of interest is carried out. Let us assume that only the one SHF source is located in the space. In this case we shell detect this source when it will hit the main lobe of the radiation pattern of the DF antenna. At that, the source bearing will be determined by the antenna position corresponding to the "global" minimum of the received signal. Below the bearing algorithm is described in detail by means of the diagram shown in Fig. 13.
Two operation modes so-called the "Search mode" and the "Bearing mode", respectively, are realized here. Under the DF operation in the "Search mode" the angular domain of the source location and its power level are determined. In the "Search mode" operation and

under the external sources failing all the LED's on the front panel of the control unit frequently blink thereby indicating an availability of both the internal equipment noises and the environment background noise. The appearance of source signal is indicated by the ignition of all the LED's and the maximum power level of the received signal with the value 0dB remain in the microcontroller memory. Any deviation of the DF antenna from this position will lead to the signal power decrease and will be accompanied by LED's switching off in pairs top-down according to the introduced normalization. During the process of the consequent space scanning within the angular domain of the revealed source, every such a scan is completed by the memorization of the maximum signal level. In other words, the following conditions hold, namely: if InpS>max; max=InpS. Thus, in the 'Search mode" operation the angular domain and the maximum signal level of the external SHF source are determined.

The parameters noted above are the initial ones for the "Bearing mode" operation. In this case a one of the upper two LED's on the working board of the control unit is shined. Let us propose that with the antenna rotation from the aforementioned initial position the received signal decreases by accompanied with the alternate LED's switching top-down so long as the lower LED goes out. These conditions correspond to the drift of antenna from the source. After that the antenna goes back to the initial position of the maximum signal reception and turns in the opposite direction (i.e., to the source). In this case the LED's will alternate switching along the appropriate branch of the symbol V on the working board of the control unit. After passing of antenna the point of the null signal reception, the LED's begin to shine in turn on the second branch of the symbol V on the working board of the control unit right up to the topmost LED. Thus, the source bearing corresponds to the antenna position when the lower LED shines on the working board of the control unit.

Let's now determine the conditions of the precise determination of the bearing angle. First of them consists in that the power level of the received signal for the antenna position corresponding the null reception must decreases to the signal level given in advance (in our case this upper level of the "global" minimum is determined by the radiation pattern of antenna and equals to -13dB). However, when holding only this condition, we can have the bearing uncertainty in view of the chaotic LED's switching between the left and right branches of the symbol V (the side lobes availability or the loss of signal at the drift of antenna from the source). In this respect the second condition is that the source must remain in the main lobe of the radiation pattern of antenna during the bearing process. Therefore, the complementary variable max_dB with the initial value of -100dB is introduced in the program and we assign in advance the condition max_dB>-5.5dB which is determined experimentally. Only in the case of the signal level exceeding -5,5dB again and subsequent its decreasing to the level <-13dB, we will observe the LED's switching from the one branch of the V-symbol to another one. It means that at first the antenna scan should be realized in the one selected direction right up to the total signal loss and only after that the antenna should turn in the opposite direction.

If the signal level (in the process of antenna scanning) becomes less than -12dB, the lower LED shines on the front panel of the control unit and with the subsequent signal level increase the LED's will be alternate shined on the another branch. It is worth noting that the lower LED goes out when the signal level becomes <-25dB. Just this condition corresponds to the signal loss. Thus, this is the lower limit of the received signal level at which all the LED's go out.

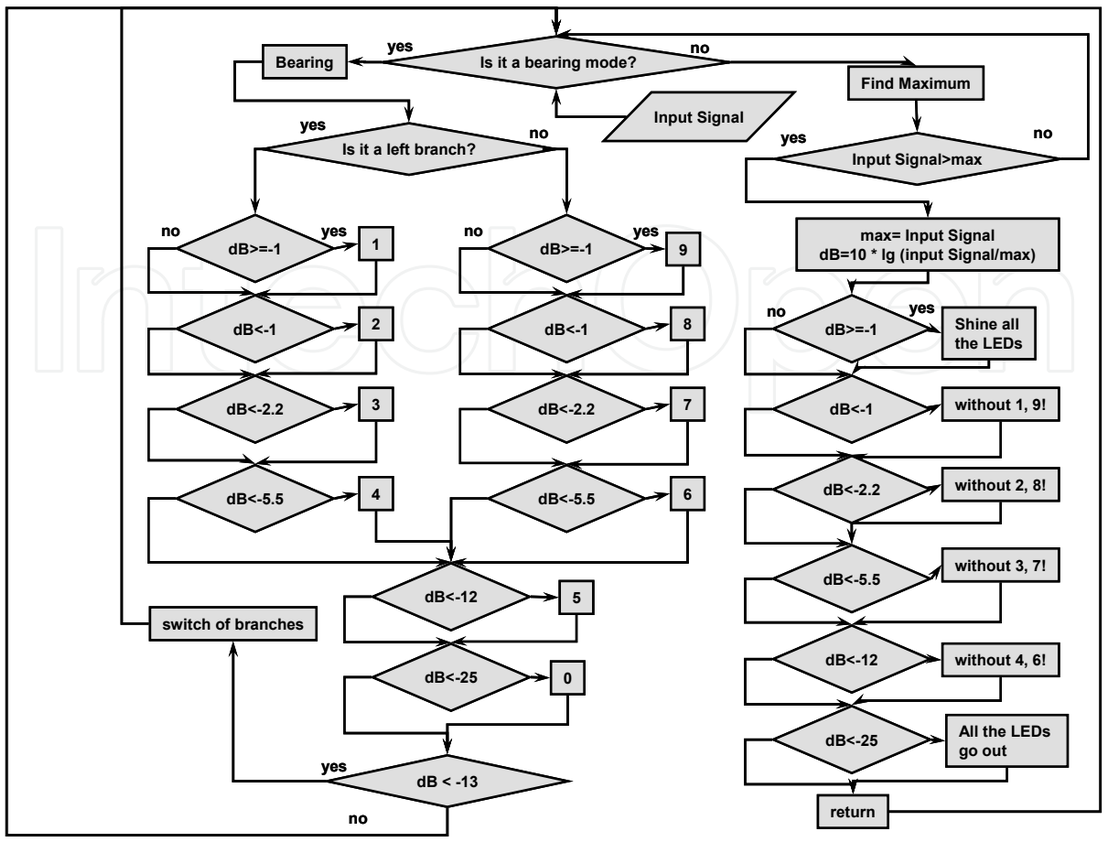

Fig. 13. Block-diagram illustrating the bearing algorithm

6. Model experiments

We have carried out a set of model experiments on the SHF source bearing by means of the aforementioned DF prototype. In these experiments we used the standard open-ended X-band waveguide as the isolated source, which was located at the distance 100m from the DF antenna (Fig. 14).

By using the algorithm noted above we have determined the direction on the SHF source with an evaluation accuracy of the source bearing equal to 2^0. We note that the noise-factor of the DF integrally (excluding the DF operation in zenith directly) averages 2 – 4dB depending on the angle of arrival.

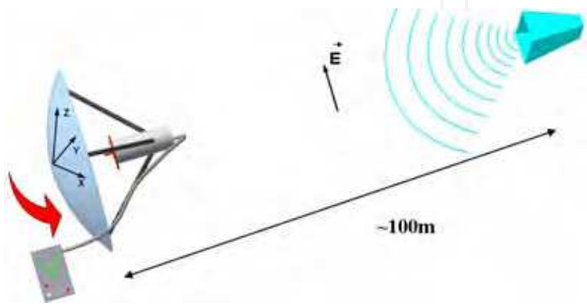

Fig. 14. Bearing the SHF source (f=10.3 GHz)

Another situation is shown in Fig. 15. In the case when the angle between two incoherent sources equals to the two beamwidths $2\theta_b$ or less, the sources bearing will not be determined correctly. In fact, one may assume that a single virtual source is located between two real sources. It is evident that we shall face the challenge like that in the case of several active SHF sources located in the analyzable space. Therefore, our further investigations will be aimed at the development of effective algorithms which allow one to solve this problem as well as to determine the source position and to improve the DF sensitivity.

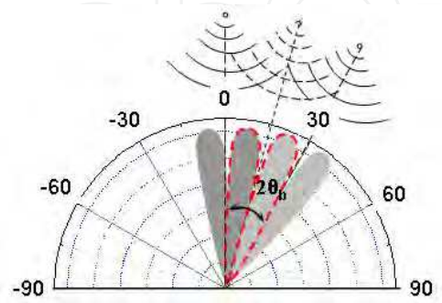

Fig. 15 Bearing of the two SHF sources operating at frequencies f_1=10.3GHz and f_2=9.2GHz, respectively

Finally, we have to take into account that the polarization of the source radiation will play a vital part in the bearing process. In spite of the fact that the DF antenna is able to receive the SHF signal with an arbitrary polarization, such an immovable antenna will be blind to the source having E_φ-polarization and moving in the same plane.

7. Conclusion

The original reflector antenna design with the cylindrical monopole antenna as a sub-reflector has been presented. The good matching of the reflector antenna to 50 Ohm feeding line has been achieved over the entire operational frequency band. The main features of the bearing algorithm have been described in detail. The capability and benefits of the proposed DF have been demonstrated by the model experiments on the external SHF source bearing. The results of model experiments with the DF prototype allow for estimating its basic characteristics:

Operational frequency band	6 – 11.5GHz
Dynamic range	50 dB
Noise factor	<3 dB
Bearing accuracy	2^0
Beamwidth	10^0
Elevation angle of peak directivity	80^0
Radiation power ratio in the antenna axis and in the radiation maximum	<-20dB
Power level of side lobes	-20dB
Cross-polarization level	<-15dB
Bearing method	“null-amplitude” technique

The proposed DF seems to be very attractive for BWLL, WLAN, and WiMAX applications.

8. References

Andrenko, A. et. al. (2006). Active Broad X-Band Circular Patch Antenna, *IEEE ANTENNAS AND WIRELESS PROPAGATION LETTERS*, Vol. 5, 2006, pp. 529-533.

Bellion, C. et. al. (2008). A New Compact Dually Polarized Direction Finding Antenna on the UHF Band, *Proceedings of the Antennas and Propagation International Symposium and USNC/URSI National Radio Science Meeting*, 526.7, July 2008.

Bu-hong, W. et. al. (2008). Ambiguity Analysis and Solution for Direction Finding of Uniform Circular Array with Mutual Coupling, *Proceedings of the Antennas and Propagation International Symposium and USNC/URSI National Radio Science Meeting*, 225.10, July 2008.

Cao, W. et. al. (2002). Modal Analysis of Rectangular Dielectric Resonator Antennas, *Proceedings of the International Symp. of Antennas,* pp.729-731, Nice (France), May 2002.

Chernobrovkin, R. et. al. (2006). Millimeter wave nondestructive testing techniques for the embedded defects characterization, *Proceedings of the «Mediterranean Microwave Symposium MMS-2006»*, pp. 216-219, Genova (Italy), September 2006.

Chernobrovkin, R. et. al. (2007). A Novel V-band Antenna for Nondestructive Testing Techniques, *Microwave and Optical Technology Letters,* Vol. 49, No. 7, Jul. 2007, pp. 1732-1735.

Chevalier, P. et. al. (2007). Highter Order Direction Finding From Arrays With Diversely Polarized antennas, *Transactions on Signals Processing*, Vol. 55, No 11, Nov. 2007.

Choi, Jun-Ho et. al. (2008). Indoor Sensor Array Test-Bed (SATB) for Direction Finding Applications at Communication-band, *Proceedings of the Antennas and Propagation International Symposium and USNC/URSI National Radio Science Meeting,* 439.7, July 2008.

Friedlander, B. & Weiss, A. (1991). Direction finding in the presence of mutual coupling, *IEEE Trans. Antenna Propag.,* Vol. 39, No. 3, Match 1991, pp.273-284.

Ivanchenko, I. et. al. (2002). Experimental Studies of X-band Leaky-wave Antenna Performances, *Microwave and Optical Technology Letters*, Vol. 35, No. 4, April 2002, pp. 281-283.

Ivanchenko, I. et. al. (2006). Effect of finite screen and monopole's height on radiation characteristics of monopole antenna, *Proceedings of the 16-th international conference on microwaves, radar and wireless communications MICON-2006*, pp.729-731, Krakov (Poland), May 2006.

Ivanchenko, I. et. al. (2007). Compact broad-band SHF direction finder for WiMax applications, *Proceedings of the 10th European Conference on Wireless Technology. EuMW/07,* pp. 316-319, Munich (Germany), October 2007.

Ivanchenko, I. et. al. (2008). Broadband SHF direction-finder, *Radioengineering,* Vol. 17, No. 2, June 2008, pp.61-65.

Jinkins, H. (1991). Small aperture radio direction finding, In: *Artech House*.

Khruslov, M. & Pazynin V. (2006). Edge effect influence on a radiation formation of the cylindrical monopole antenna, *Proceedings of the «Mathematical methods in electromagnetic theory MMET-2006»*, pp. 178-180, Kharkov (Ukraine), June 2006.

Kwai, K. et. al. (2008). Robust Symmetrical Number System Direction Finding Arrays with Virtual Spacing, *Proceedings of the Antennas and Propagation International Symposium, and USNC/URSI National Radio Science Meeting,* 237.3, July 2008.

Pace, P. et al. (2001). High Resolution Phase Sampled Interferometry Using Symmetrical Number Systems, *IEEE Transactions on Antennas and Propagation,* Vol. 49, No. 10, October 2001, pp. 1411-1423.

Peyrot-Solis, M. et. al. (2005). State of the Art in Ultra Wideband Antennas, *Proceedings of the 2nd International Conference on Electrical and Electronics Engineering and XI Conference on Electrical Engineering* 2005.

Poisel, R. (2005). Electronic Target Location Methods, In: *Artech House*.

Radionov, S. et. al. (2007). Broadband SHF direction-finder, *Proceedings of the 19th International Conference on Applied Electromagnetics and Communications*, pp. 67-70, Dubrovnik (Croatia), October 2007.

Sarkis, R. et. al. (2008). Amplitude and Phase Correction of the Radiation Pattern in Compact Planar Antenna Array for Direction Finding Applications, *Proceedings of the Antennas and Propagation International Symposium and USNC/URSI National Radio Science Meeting*, 435.3, July 2008.

Schantz, H. (2004). A Brief History of UWB Antennas, *Proceedings of the IEEE A&E Systems Magazine,* April 2004.

Schmidt, R. (1986). Multiple emitter location and signal parameter estimation, *IEEE Trans. on Antennas and Propagation,* Vol. AP-345, No. 3, Mar. 1986, pp. 276-280.

See, C. & Poh, B. (1999). Parametric sensor array calibration using measured steering vectors of uncertain locations. *IEEE Trans. Signal Processing,* Vol.47, No.4, April 1999, pp.1133-1137.

Xiaobo, V. & Zhenghe, R. (2002). A single channel correlative interferometer direction finder using VXI receiver, *Proceedings of the Int, Conf. on Microwave and Millimeter wave Technology,* Aug. 2002.

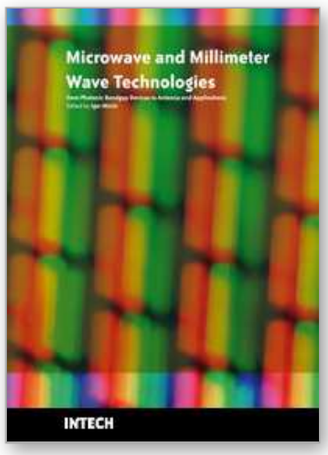

Microwave and Millimeter Wave Technologies from Photonic Bandgap Devices to Antenna and Applications

Edited by Igor Minin

ISBN 978-953-7619-66-4
Hard cover, 468 pages
Publisher InTech
Published online 01, March, 2010
Published in print edition March, 2010

The book deals with modern developments in microwave and millimeter wave technologies, presenting a wide selection of different topics within this interesting area. From a description of the evolution of technological processes for the design of passive functions in milimetre-wave frequency range, to different applications and different materials evaluation, the book offers an extensive view of the current trends in the field. Hopefully the book will attract more interest in microwave and millimeter wave technologies and simulate new ideas on this fascinating subject.

How to reference

In order to correctly reference this scholarly work, feel free to copy and paste the following:

Sergey Radionov, Igor Ivanchenko, Maksym Khruslov, Aleksey Korolev and Nina Popenko (2010). Microwave and Millimeter Wave Technologies A New X-Band Mobile Direction Finder, Microwave and Millimeter Wave Technologies from Photonic Bandgap Devices to Antenna and Applications, Igor Minin (Ed.), ISBN: 978-953-7619-66-4, InTech, Available from: http://www.intechopen.com/books/microwave-and-millimeter-wave-technologies-from-photonic-bandgap-devices-to-antenna-and-applications/microwave-and-millimeter-wave-technologies-a-new-x-band-mobile-direction-finder

INTECH
open science | open minds

InTech Europe
University Campus STeP Ri
Slavka Krautzeka 83/A
51000 Rijeka, Croatia
Phone: +385 (51) 770 447
Fax: +385 (51) 686 166
www.intechopen.com

InTech China
Unit 405, Office Block, Hotel Equatorial Shanghai
No.65, Yan An Road (West), Shanghai, 200040, China
中国上海市延安西路65号上海国际贵都大饭店办公楼405单元
Phone: +86-21-62489820
Fax: +86-21-62489821

IntechOpen